

Exploitation of Synchrotron Radiation Photoionization Mass Spectrometry in the Analysis of Complex Organics in Interstellar Model Ices

Cheng Zhu, Hailing Wang, Iakov Medvedkov, Joshua Marks, Minggao Xu, Jiuzhong Yang, Tao Yang,* Yang Pan,* and Ralf I. Kaiser*



Cite This: *J. Phys. Chem. Lett.* 2022, 13, 6875–6882



Read Online

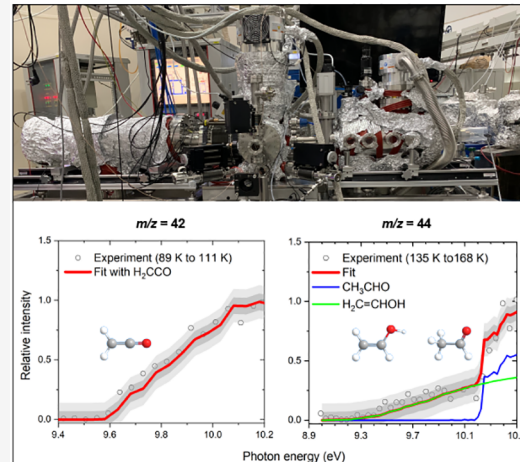
ACCESS |

Metrics & More

Article Recommendations

Supporting Information

ABSTRACT: Unravelling the generation of complex organic molecules (COMs) on interstellar nanoparticles (grains) is essential in establishing predictive astrochemical reaction networks and recognizing evolution stages of molecular clouds and star-forming regions. The formation of COMs has been associated with the irradiation of interstellar ices by ultraviolet photons and galactic cosmic rays. Herein, we pioneer the first incorporation of *synchrotron vacuum ultraviolet photoionization reflectron time-of-flight mass spectrometry* (SVUV-PI-ReTOF-MS) in laboratory astrophysics simulation experiments to afford an isomer-selective identification of key COMs (ketene ($\text{H}_2\text{C}=\text{CO}$); acetaldehyde (CH_3CHO); vinyl alcohol ($\text{H}_2\text{C}=\text{CHOH}$)) based on photoionization efficiency (PIE) curves of molecules desorbing from exposed carbon monoxide–methane ($\text{CO}-\text{CH}_4$) ices. Our results demonstrate that the SVUV-PI-ReTOF-MS approach represents a versatile, rapid methodology for a comprehensive identification and explicit understanding of the complex organics produced in space simulation experiments. This methodology is expected to significantly improve the predictive nature of astrochemical models of complex organic molecules formed abiotically in deep space, including biorelated species linked to the origins-of-life topic.



Complex organic molecules (COMs), carbon-containing compounds with six or more atoms such as alcohols (ROH), aldehydes (RCHO), and ketones (RCOR') (R and R' representing alkyl groups), have been found to be ubiquitous in the interstellar medium (ISM).^{1–3} Untangling the abiotic generation mechanisms of key COMs is of fundamental importance to the astrochemistry, physical chemistry, astrophysics, and astrobiology communities.^{4–6} In particular, a detailed understanding of the formation of structural isomers, molecules with identical chemical formula but distinct connectivities of atoms, of COMs like acetaldehyde (CH_3CHO) and its enol isomer vinyl alcohol ($\text{H}_2\text{CCH}(\text{OH})$) is of vital significance because they are recognized as tracers of interstellar physical and chemical conditions and to evaluate reaction processes in molecular clouds—the nurseries of stars and planetary systems—and star-forming regions through astrochemical modeling.^{7,8} COMs carrying multiple functional groups such as amino acids α -amino-n-butyric acid ($\text{CH}_3\text{CH}_2\text{CH}(\text{NH}_2)\text{COOH}$) and glutamic acid ($\text{HOOCCH}_2\text{CH}_2\text{CH}(\text{NH}_2)\text{COOH}$) and sugars like ribose ($\text{C}_5\text{H}_{10}\text{O}_5$) and arabinose ($\text{C}_5\text{H}_{10}\text{O}_5$) have been identified in the Murchison meteorite, a carbonaceous chondrite.^{9–11} Carbonaceous chondrites are contemplated as the most

primitive leftovers from the early Solar System and carry unique information on the chemical evolution history of our Solar System.¹² Consequently, an understanding of the origin of COMs in these meteorites is critical because they resemble prebiotic time capsules.

Therefore, despite the critical role of COMs in unraveling the astrochemical evolution of the ISM, the fundamental pathways leading to the formation of COMs still has not been fully untangled.^{13,14} The synthesis of COMs has been connected to the interaction of ionizing radiation (e.g., galactic cosmic rays (GCRs) and ultraviolet (UV) photons)^{5,6} with low-temperature (10 K) ices coated on interstellar dusts.^{15–20} Laboratory works found that processing of interstellar analogue ices with ionizing radiation provides an extensive spectrum of COMs, including the sugar-related glycolaldehyde ($\text{HCO}-\text{CH}_2\text{OH}$),^{21–24} amino acids,^{25–27} and even dipeptides^{28,29} along with alkylphosphonic acids^{30,31} and glycerolphosphates.²⁰ Interstellar ices mainly consist of simple molecules, e.g., water (H_2O), methanol (CH_3OH), methane (CH_4),

Received: May 29, 2022

Accepted: July 18, 2022

formaldehyde (H_2CO), carbon monoxide (CO), and ammonia (NH_3).² The densest parts of these molecular clouds collapse to generate star-forming regions. In these environments, heating increases temperatures up to 300 K and (partially) sublimes the COMs into the gas phase. The gaseous molecules can be detected by radio telescopes.^{32–35} A detailed understanding of the generation mechanisms of key COMs requires new technology exploring creative and transformative concepts for carrying out high-level innovative and systematic experimental studies to identify and then to extract the underlying formation pathways of COMs in astrophysically relevant interstellar ices.

For the last decades, the astrochemistry and laboratory astrophysics communities have exploited nanometer-thick (mixtures of) model ices deposited on low-temperature targets (5–20 K)^{6,19} and exposed them to ionizing radiation such as ultraviolet (UV) light, X-rays, protons, helium nuclei, and electrons.^{4,6,17–20} These systems served as proxies of real interstellar ices condensed on low-temperature (10 K) interstellar dusts and simulated the interaction with the internal UV photons and GCRs. During the processing by ionizing radiation, these ices were monitored predominantly via Fourier-transform infrared spectroscopy (FTIR),^{15–20} ultraviolet-visible (UV-vis) spectroscopy,^{36,37} and Raman spectroscopy,^{38–40} thus elucidating the formation of small molecules and of functional groups of COMs. This phase is often followed by annealing the irradiated samples to 300 K (temperature-programmed desorption phase; TPD) and probing the subliming molecules exploiting *hard* electron impact ionization quadrupole mass spectrometry (EI-QMS),^{41–43} millimeter and submillimeter spectroscopy (MM/subMMS),^{44,45} and soft photoionization via single-photon (PI) or resonance-enhanced multiphoton ionization (REMPI) coupled with reflectron time-of-flight mass spectrometry (ReTOF-MS).^{31,46–51} Traditional FTIR nicely aided in investigating the synthesis of simple species such as carbon monoxide (CO) and carbon dioxide (CO_2);^{52,53} this technique, however, exposed critical limitations in identifying *individual* species of complex organics because of overlapping fundamentals in the infrared regime of the electromagnetic spectrum. Likewise, severe fragmentation of molecular ions of complex organics induced by EI severely limits the application of EI-QMS in the identification of COMs and in particular of structural isomers. Recently, gas-phase MM/subMMS has been proposed for distinguishing structural isomers.^{44,45} However, this technique relies on molecules carrying a permanent dipole moment and hence lacks versatility. The recently implemented soft photoionization in conjunction with ReTOF-MS affords an extremely sensitive tool in discriminating *structural isomers* such as methanediol ($\text{CH}_2(\text{OH})_2$) and methyl peroxide (CH_3COOH).⁵¹ This is accomplished by comparing the TPD curves of distinct target molecules at different photon energies chosen to selectively ionize specific isomers based on their distinct ionization energies (IEs).^{6,54} However, this method requires a time-intensive repetition of the same irradiation experiment along with extensive baking periods between experiments to achieve ultrahigh vacuum in the setup at *each* photon energy (PE) to be investigated. Only recently, this approach has been extended to determine *ionization thresholds* of molecules subliming from exposed model ices in the TPD phase through the use of photoionization efficiency (PIE) curves within a single experiment, which report the ion counts at a well-defined mass-to-charge

(*m/z*) ratio versus the photon energy.⁵¹ However, the limited tunable range of only 0.1–0.2 eV did not allow the identification of complex mixtures of structural isomers of COMs during the TPD phase of the irradiated low temperature samples—a critical versatility exploited in the elucidation of the isomer-selective formation of polycyclic aromatic hydrocarbons (PAHs) in high-temperature gas-phase chemical reactors coupled to vacuum ultraviolet (VUV) beamlines of synchrotrons.⁵⁵ Therefore, the exploitation of VUV light in the collection of PIE curves and hence identifying structural isomers of COMs of often astrobiologically relevant molecules from subliming interstellar analogue ices has been challenging and just scratched the surface.

Herein, by exploiting acetaldehyde (CH_3CHO) along with its enol tautomer vinyl alcohol ($\text{H}_2\text{C}=\text{CHOH}$) as a benchmark (Figure 1), we pioneer the incorporation of

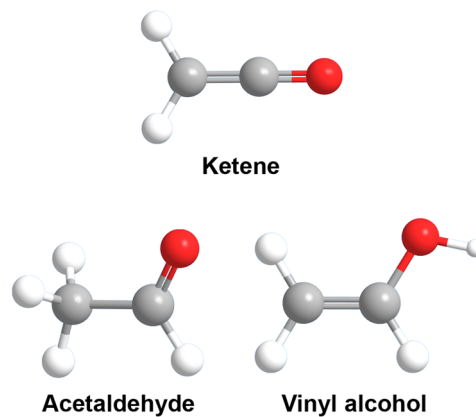


Figure 1. Molecular structures of ketene ($\text{H}_2\text{C}=\text{CO}$) and acetaldehyde (CH_3CHO) along with its enol tautomer vinyl alcohol ($\text{H}_2\text{C}=\text{CHOH}$).

synchrotron vacuum ultraviolet photoionization reflectron time-of-flight mass spectrometry (SVUV-PI-ReTOF-MS) in laboratory astrophysics simulation experiments (Figures S1 and S2) to probe the desorbing molecules during the TPD phase of interstellar model ices of carbon monoxide–methane (CO– CH_4) processed at 5.0 ± 0.1 K at 10^{-11} Torr by energetic electrons simulating secondary electrons generated during the GCRs of these interstellar ices²¹ over the typical lifetime (a few 10^6 years) of molecular clouds. Single-photon synchrotron vacuum ultraviolet radiation represents a unique ionization source characterized by soft ionization ideally without fragmentation of the molecular ion near the ionization threshold, broad tunability from 7 to 11 eV^{56–58} covering the range of the ionization energies of COMs, and high energy resolution of 0.05 eV. These features entirely circumvent time-intensive repetition of the laboratory simulation experiments by rapidly scanning the SVUV energies and allow for the first time the collection of PIE curves of all molecules subliming from the processed interstellar model ices in the TPD phase simultaneously. The comprehensive and unambiguous identification of COMs hence constrains the fundamental processes linked to the formation of biologically relevant COMs identified in the ISM and in meteorites. These abiotically formed molecules could have been transported to early Earth, thus making available the raw materials for early biochemical evolution.

To demonstrate the unique potential of the SVUV-PI-ReTOF-MS technique, we report on the *isomer-selective* identification of ketene ($\text{H}_2\text{C}=\text{CO}$) along with the acetaldehyde–vinyl alcohol ($\text{CH}_3\text{CHO}-\text{H}_2\text{C}=\text{CHOH}$) isomer pair in the TPD phase of processed apolar carbon monoxide–methane ($\text{CO}-\text{CH}_4$) model ices (Table S1). Both the carbon monoxide and methane precursors have been identified in interstellar ices at concentrations of 3–26% and 1–5% with respect to water, respectively.² The experimental irradiation dose is $0.17 \pm 0.03 \text{ eV amu}^{-1}$ ($4.7 \pm 0.8 \text{ eV}$ per CO molecule and $2.7 \pm 0.4 \text{ eV}$ per CH_4 molecule) (Table S2), representing radiation exposures in molecular clouds⁵⁹ over a few 10^6 years. In this protocol, the SVUV energy was first kept at 10.49 eV to monitor the temperature-dependent mass spectra of the desorbing species from the irradiated samples (Figure 2), thus presenting a global overview of the molecular

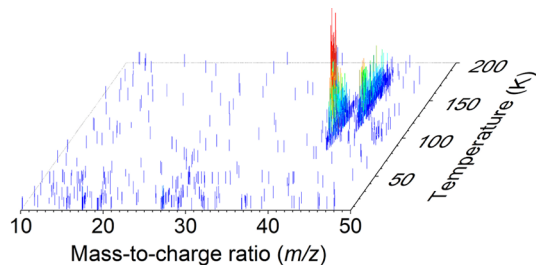


Figure 2. Synchrotron vacuum ultraviolet photoionization reflectron time-of-flight mass spectrometry (SVUV-PI-ReTOF-MS) data recorded during the temperature-programmed desorption (TPD) phase of a processed carbon monoxide–methane ($\text{CO}-\text{CH}_4$) ice.

formulas of species synthesized. Thereafter, the SVUV light is tuned from 9.00 to 10.49 eV in 0.05 eV intervals to record photon energy and temperature-dependent mass spectra in the TPD phase. By normalizing the TPD profiles for all m/z ions collected during the scan of the SVUV energies with respect to the profiles at 10.49 eV and to photon flux, these data will then be converted to distinct PIE curves, which can be compared to PIE data from the literature.^{60,61} As shown in Figures 2 and S3, four distinct mass-to-charge ratios were detected, *i.e.*, two dominant peaks at $m/z = 42$ and 44 along with two less intense signals at $m/z = 43$ and 45. The corresponding TPD profiles and PIE curves are depicted in Figures 3 and 4 along with Figure S4. The experimental PIE curves are shifted by 0.02 eV because of the decrease of the IEs by the electric field of the extractor plates (Figure S5).^{62–64}

$m/z = 42$ and 43. At PE = 10.49 eV, the TPD profile of $m/z = 42$ exhibits a sublimation peak between 80 and 130 K with a maximum at about 100 K (Figure 3a). In principle, the signal can be associated with $\text{C}_2\text{H}_2\text{O}$ and/or C_3H_6 isomers. The corresponding PIE curve can be utilized to determine the carrier(s) of this signal (Figure 3b). Overall, the experimental data correlates nicely with the reference PIE curve of ketene ($\text{H}_2\text{C}=\text{CO}$).⁶¹ The onset of the ion counts of $9.60 \pm 0.05 \text{ eV}$ is in good agreement with the adiabatic IE of ketene of $9.617 \pm 0.003 \text{ eV}$.⁶⁵ The inclusion of additional isomers, *e.g.*, ethynol (HCCOH , IE = $10.03 \pm 0.03 \text{ eV}$),⁶⁶ propene (C_3H_6 , IE = $9.73 \pm 0.01 \text{ eV}$),⁶⁵ and cyclopropane ($\text{c-C}_3\text{H}_6$, IE = $9.86 \pm 0.04 \text{ eV}$),⁶⁵ would alter the shape of the PIE considerably and cannot replicate the experimental data. Therefore, we conclude that within the error limits, ketene ($\text{H}_2\text{C}=\text{CO}$) is the main contributor of the signal at $m/z = 42$. Note that signal at $m/z =$

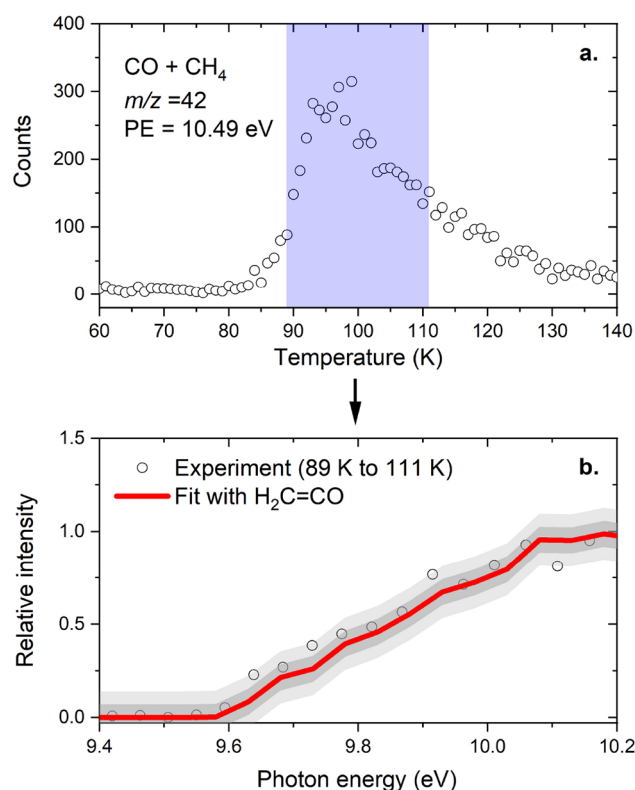


Figure 3. SVUV-PI-ReTOF-MS data at $m/z = 42$. (a) $m/z = 42$ signal detected during the TPD phase of the irradiated carbon monoxide–methane ($\text{CO}-\text{CH}_4$) ice at a photon energy of 10.49 eV. (b) Photoionization efficiency (PIE) curve for the species linked to $m/z = 42$ (open cycles) recorded from 89 to 111 K (light-blue shaded region in panel a). The red line shows the fit of the reference PIE curve of ketene ($\text{H}_2\text{C}=\text{CO}$) to the experimental $m/z = 42$ data. The uncertainties in the fit are noted with dark-gray (1σ) and light-gray (2σ) shaded regions.

43 can be linked to the ^{13}C analogue of ketene ($\text{H}_2\text{C}=\text{CO}$) as its TPD and PIE profiles overlap with that of $m/z = 42$, but with much weaker intensity of only $1.6 \pm 0.3\%$ accounting for naturally existing ^{13}C (1.1%) and two carbon atoms in ketene.

$m/z = 44$ and 45. The molecular ions of $\text{C}_2\text{H}_4\text{O}$ and C_3H_8 isomers can be linked to the signal at $m/z = 44$. At PE = 10.49 eV, two sublimation events peaking at 122 and 150 K are observed (Figure 4a). These can be attributed to acetaldehyde (CH_3CHO ; IE = $10.2290 \pm 0.0007 \text{ eV}$) and/or vinyl alcohol ($\text{H}_2\text{C}=\text{CHOH}$; IE = $9.33 \pm 0.01 \text{ eV}$), but not ethylene oxide (IE = $10.56 \pm 0.01 \text{ eV}$) and propane ($\text{CH}_3\text{CH}_2\text{CH}_3$, IE = $10.94 \pm 0.05 \text{ eV}$),⁶⁵ which cannot be ionized at 10.49 eV. Likewise, photons at 10.49 eV cannot ionize carbon dioxide (CO_2) either (IE = $13.777 \pm 0.001 \text{ eV}$).⁶⁵ The PIE curve of $m/z = 44$ extracted from the early section covering 113–132 K reveals that these data match exceptionally well with the reference PIE curve for acetaldehyde (CH_3CHO) (Figure 4b). On the other hand, the PIE curve extracted during the sublimation from 135 to 168 K can be reproduced only by a linear combination of reference PIE curves for vinyl alcohol ($\text{H}_2\text{C}=\text{CHOH}$) and acetaldehyde (CH_3CHO) (Figure 4c).⁶⁰ The onset of the ion counts at $9.30 \pm 0.05 \text{ eV}$ agrees nicely with the IE of vinyl alcohol of $9.33 \pm 0.01 \text{ eV}$.⁶⁵ The contribution of vinyl alcohol to the signal up to 10.25 eV is essential. From 10.25 to 10.49 eV, the incorporation of acetaldehyde is imperative to fit the detected data. The onset

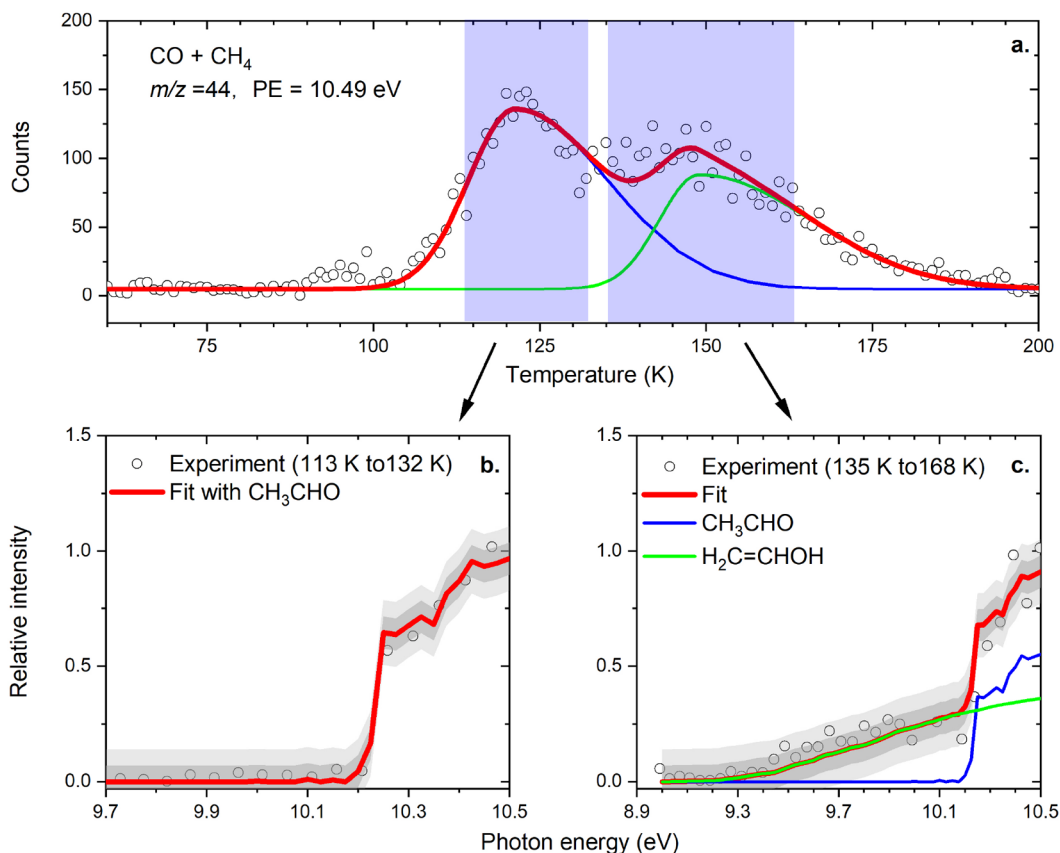


Figure 4. SVUV-PI-ReTOF-MS data at $m/z = 44$. (a) $m/z = 44$ signal (open circles) detected during the TPD phase of the irradiated carbon monoxide–methane ($\text{CO}-\text{CH}_4$) ices at photon energy of 10.49 eV. The data are fitted with two bi-Gaussian peaks (blue and green lines). The red line corresponds to the sum of the deconvoluted fittings. (b) PIE curve for the species linked to $m/z = 44$ (open circles) recorded from 113 to 132 K (left light-blue shaded region in panel a). The red line shows the fit of the reference PIE of acetaldehyde (CH_3CHO) to the experimental $m/z = 44$ data. (c) PIE curve for the species linked to $m/z = 44$ (open circles) recorded from 135 to 168 K (right light-blue shaded region in panel a). The red line shows the fit of the reference PIE curves of acetaldehyde (CH_3CHO) (blue line) and vinyl alcohol ($\text{H}_2\text{C}=\text{CHOH}$) (green line) to the experimental data at $m/z = 44$. The uncertainties in the fit are noted with dark-gray (1σ) and light-gray (2σ) shaded regions.

of 10.25 ± 0.05 eV matches nicely with the IE of acetaldehyde of 10.2290 ± 0.0007 eV.⁶⁵ These results provide compelling evidence of an isomer-selective identification of acetaldehyde and vinyl alcohol. Considering the ratio of the deconvoluted peaks of acetaldehyde/vinyl alcohol = $(1.45 \pm 0.12)/1$ and the experimental photoionization cross sections of acetaldehyde ($(7.4 \pm 1.9) \times 10^{-22} \text{ m}^2$) and vinyl alcohol ($(9.7 \pm 2.4) \times 10^{-22} \text{ m}^2$) at 10.49 eV,⁶⁶ the exact branching ratio is calculated to be acetaldehyde/vinyl alcohol = $(1.90 \pm 0.57)/1$. The data at $m/z = 45$ data can be linked to ^{13}C -substituted acetaldehyde and vinyl alcohol, but they are too weak to be deconvoluted. It should be highlighted that ion counts at m/z from 42 to 45 were not identified in a blank experiment carried out under the same conditions but without electron irradiation of ices, which demonstrates that the detected species in the irradiation experiments are due to the electron processing of the samples but are not formed in the gas phase via ion–molecule reactions.

In summary, we pioneered the incorporation of *synchrotron vacuum ultraviolet photoionization reflectron time-of-flight mass spectrometry* (SVUV-PI-ReTOF-MS) in laboratory astrophysics simulation experiments. As a proof-of-concept, the isomer-specific synthesis and detection of two structural isomers of COMs, acetaldehyde (CH_3CHO) and vinyl alcohol ($\text{H}_2\text{C}=\text{CHOH}$), along with ketene ($\text{H}_2\text{C}=\text{CO}$) in electron-processed

astrophysically relevant carbon monoxide–methane ices, demonstrated the potential and versatility of the exploitation of the SVUV-PI-ReTOF-MS technique to record and to exploit PIE curves through photoionization of the desorbing molecules during the TPD phase of exposed astrophysically relevant ices. The comparison of experimental PIE curves with reference PIE curves of the individual structural isomers was verified to be an ideal approach in untangling the chemical complexity of complex mixtures of organics prepared under realistic space simulation conditions in the laboratory over the lifetime of cold molecular clouds (a few 10^6 years). The unique characteristics of this technique in terms of a fragment-free soft photoionization and facile tunability of the VUV energy together with the capability of collecting the associated PIE curves affords an exciting approach to explicitly discriminate complex organic molecules and their isomers, in particular *in situ*. This methodology overcomes previous limitations of traditional EI-QMS (overlapping mass fragmentation), FTIR (overlapping absorptions of organics with identical functional groups), and MM/subMMS spectroscopy (limited to molecules of nonzero dipole moments) and boosts the proficiency of space simulation experiments to the next level that is able to efficiently examine complex mixtures of organics synthesized in the interaction of ionizing radiation with astrophysically relevant ices under various interstellar conditions, e.g., wide

range of temperatures, radiation types and doses, and ice phases, and to assist the establishment of comprehensive astrochemical reaction models. This is of particular significance to decipher the origin of biorelated species linked to the origins of life theme, thus critically aiding our understanding of the rapidly growing observational data collected in the era of the Atacama Large Millimeter/submillimeter Array (ALMA)^{67,68} and Five-hundred-meter Aperture Spherical Telescope (FAST) through a comparison of data from astronomical observations with prospective inventories of complex organics synthesized and detected in space simulation experiments exploiting the SVUV-PI-ReTOF-MS.

METHODS

Simulation Experiment: Chamber. The experiments were performed at the Shanghai-Hawaii-Hefei Advanced Research Center for Astrochemistry utilizing the Mass Spectrometry Beamline (BL04B) of National Synchrotron Radiation Laboratory (NSRL) (Figure S1). This novel surface science machine consists of a contamination-free ultrahigh vacuum chamber, which is pumped to a few 10^{-11} Torr by a magnetically levitated turbo molecular pump (Osaka Vacuum, TG1300M), backed by a turbomolecular pump (Osaka Vacuum, TG420M) and dry-compression multistage roots pumps (Leybold, Ecodyn 40 Plus). Within the chamber, a polished silver substrate is attached to an oxygen-free high thermal conductivity (OFHC) copper coldfinger, which is interfaced to a two-stage closed cycle helium refrigerator (Sumitomo Heavy Industries, RDK-41SE) to obtain temperatures as low as 4.8 ± 0.1 K. The silver substrate can be vertically moved and horizontally rotated via using an ultrahigh-vacuum compatible bellow (McAllister, BLT106) and a doubly differentially pumped rotary platform (Thermionics Vacuum Products, RNN-600/FA/MCO), respectively. The substrate temperature was measured by a cryogenic temperature sensor (Lakeshore, DT-470) and regulated (from 5 to 300 K) by a programmable temperature controller (Lakeshore, Model 336) with a precision of ± 0.1 K.

Simulation Experiment: Deposition. The silver target was first cooled to 5.0 ± 0.1 K and moved to the deposition position. Carbon monoxide (CO, Sigma-Aldrich, 99.99%) and methane (CH₄, Specialty Gases of America, 99.9%) were mixed in a gas mixing chamber and deposited onto the silver target through a glass capillary array (main chamber pressure at 5×10^{-8} Torr, 30 min deposition) to prepare ice mixtures of CO/CH₄ = $(1.0 \pm 0.2)/1$. The overall ice thicknesses were determined utilizing laser interferometry with a He-Ne 632.8 nm laser (CVI Melles Griot; 25-LHP-230).⁶⁹ In detail, the laser light was directed on to the sample target at an incidence angle of 2° and reflected to a photodiode (Thorlabs, SM1PD1A) connected to a picoammeter (Keithley 6485), which can record the interference patterns of the fraction of the light that reflects off the surface of the ice with the fraction that penetrates the ice and reflects off the substrate. With the interferogram and the refractive indexes of $n_{\text{CO}} = 1.25 \pm 0.03$ and $n_{\text{CH}_4} = 1.34 \pm 0.04$, the ice thickness was calculated to be 500 ± 50 nm.

Simulation Experiment: Irradiation. After the deposition, the target was translated to the irradiation position and isothermally irradiated with 5 keV electrons (SPECS GmbH, eq 22/35 electron source) at an angle of 70° to the ice surface normal; two experiments were conducted at 5 K at currents of 30 nA and 0 nA (blank experiment) for 1 h. Exploiting the

CASINO 2.42 simulation software,⁷⁰ the average penetration depth of the electrons was estimated to be 370 ± 40 nm (Table S2), which is less than the 500 ± 50 nm ice thickness; this avoids an interaction between the electrons and the silver wafer. As shown in Table S2, the irradiation doses at 30 nA are 4.7 ± 0.8 eV per CO molecule and 2.7 ± 0.4 eV per CH₄ molecule.

Simulation Experiment: Temperature-Programmed Desorption (TPD). After the irradiation, the targets were rotated to the TPD position and then annealed from 5 to 300 K at a rate of 0.5 K min^{-1} (TPD phase). During this phase, the subliming molecules were monitored exploiting *synchrotron vacuum ultraviolet photoionization reflectron time-of-flight mass spectrometry* (SVUV-PI-ReTOF-MS) (Figure S1). Synchrotron radiation from a bending magnet at the BL04B beamline of NSRL was monochromatized with a homemade 1200 lines per millimeter blazed grating. This grating covers the photon energy from 5.0 to 11.8 eV with a lithium fluoride (LiF) window having an energy resolving power of about 500 ($E/\Delta E$). The average photon flux is in the magnitude of 10^{11} photons per second. A silicon photodiode (SXUV-100, Opto Diode Corporation) was utilized to measure the photon flux. The ionized species were then mass analyzed using an ReTOF mass spectrometer (Jordan TOF Products, Inc.) operating with $3 \mu\text{s}$ extraction pulses, which were generated by a pulse delay generator (Quantum Composers, 9528) operating at 30 kHz repetition rate. The schematic and optimized voltages of the ReTOF mass spectrometer are shown in Figure S1. The signal was amplified and discriminated with an F-100T amplifier-discriminator (Advanced Research Instruments Corporation) and recorded by a multichannel scalar (FAST ComTec, P7889) equipped in an industrial personal computer. A single ReTOF mass spectrum represents the accumulation of 3 600 000 sweeps in a 4 ns bin width, which corresponds to a data collection time of 120 s in a temperature increase of 1 K.

Simulation Experiment: Calibration. The SVUV-PI-ReTOF-MS was calibrated by introducing deuterium (D₂), methane (CH₄), and trifluoriodomethane (CF₃I) gases into the main chamber and utilizing 11.00 eV photons along with high harmonics as photoionization source. The high harmonics can fragmentize molecular ions CH₄⁺ ($m/z = 16$) and CF₃I⁺ ($m/z = 196$) generating CH₃⁺ ($m/z = 15$), CF⁺ ($m/z = 31$), CF₃⁺ ($m/z = 69$), I⁺ ($m/z = 127$), and CF₂I⁺ ($m/z = 177$) ions. The fit curve of the mass-to-charge ratio (m/z) and the time-of-flight (TOF) of ions was achieved by fitting polynomials up to the second order, *i.e.*, $m/z = (3.1304 \times 10^{-8})(\text{TOF})^2 - (8.0393 \times 10^{-6})\text{TOF} + 6.8426 \times 10^{-2}$.

Limit of Detection. We measured the limit of detection (LOD) of the SVUV-PI-ReTOF-MS at photon energy of 10.49 eV for propene (C₃H₆). The LOD was determined by slowly introducing C₃H₆ to the main chamber via a gas-dosing valve and recording mass spectrum. Once the signal-to-noise ratio of molecular ions C₃H₆⁺ ($m/z = 42$) reached greater than 3, the corresponding pressure of C₃H₆ was converted to a gas density (*i.e.*, LOD)⁴⁴ exploiting the ideal gas law. The LOD was calculated to be $(2.0 \pm 0.2) \times 10^7$ molecules cm⁻³, which is about 2 orders of magnitude lower than that of millimeter and submillimeter spectroscopy (MM/subMMS, LOD in the range of 1.1×10^9 to 3.1×10^9 molecules cm⁻³ for H₂O and CH₃OH).⁴⁴ In addition, MM/subMMS relies on molecules carrying a permanent dipole moment, which limits the versatility of this technique.

Simulation Experiment: Photoionization Efficiency (PIE) Curves. In the TPD phase, SVUV was tuned from 9.00 to 10.49 eV with 0.05 eV intervals to record photon energy and temperature-dependent mass spectra. PIE curves of all detected molecules were generated via normalizing the TPD profiles recorded during scanning the SVUV energy with respect to the TPD profiles at 10.49 eV and to photon flux yields, which report the intensities of ions at specific mass-to-charge ratios as a function of the photon energy. The measured PIE curves need to be shifted by 0.02 eV as shown in the calibration experiment with pure propene (C_3H_6) (Figure S5) because of the electric field of ion optics.^{62–64}

■ ASSOCIATED CONTENT

§ Supporting Information

The Supporting Information is available free of charge at <https://pubs.acs.org/doi/10.1021/acs.jpcllett.2c01628>.

SIMION simulation, schematics of the experimental setup (Figure S1), mass calibration curve (Figures S2), integrated mass spectrum (Figure S3), $m/z = 43$ signal (Figure S4), photoionization efficiency (PIE) curve correction (Figure S5), list of experiments (Table S1), and irradiation dose (Table S2) ([PDF](#))

■ AUTHOR INFORMATION

Corresponding Authors

Tao Yang – *State Key Laboratory of Precision Spectroscopy, East China Normal University, Shanghai 200062, P.R. China; Collaborative Innovation Center of Extreme Optics, Shanxi University, Taiyuan, Shanxi 030006, P.R. China; Email: tyang@lps.ecnu.edu.cn*

Yang Pan – *National Synchrotron Radiation Laboratory, University of Science and Technology of China, Hefei 230029, P.R. China; orcid.org/0000-0002-9360-3809; Email: panyang@ustc.edu.cn*

Ralf I. Kaiser – *Department of Chemistry, University of Hawai'i at Mānoa, Honolulu, Hawaii 96822, United States; orcid.org/0000-0002-7233-7206; Email: ralfk@hawaii.edu*

Authors

Cheng Zhu – *Department of Chemistry, University of Hawai'i at Mānoa, Honolulu, Hawaii 96822, United States*

Hailing Wang – *State Key Laboratory of Precision Spectroscopy, East China Normal University, Shanghai 200062, P.R. China; orcid.org/0000-0002-6976-8806*

Iakov Medvedkov – *Department of Chemistry, University of Hawai'i at Mānoa, Honolulu, Hawaii 96822, United States*

Joshua Marks – *Department of Chemistry, University of Hawai'i at Mānoa, Honolulu, Hawaii 96822, United States*

Minggao Xu – *National Synchrotron Radiation Laboratory, University of Science and Technology of China, Hefei 230029, P.R. China*

Jiuzhong Yang – *National Synchrotron Radiation Laboratory, University of Science and Technology of China, Hefei 230029, P.R. China; orcid.org/0000-0002-7076-3412*

Complete contact information is available at:

<https://pubs.acs.org/10.1021/acs.jpcllett.2c01628>

Author Contributions

C.Z., H.W., and I.M. contributed equally to this work.

Notes

The authors declare no competing financial interest.

■ ACKNOWLEDGMENTS

This work was conducted under a Memorandum of Understanding (MOU) between the East China Normal University (ECNU), the University of Hawai'i at Mānoa (UHM), and the National Synchrotron Radiation Laboratory (NSRL) at the University of Science and Technology of China (USTC). T.Y. acknowledges the support from the National Natural Science Foundation of China (Grant No. 12034008), the Young Top-Notch Talent Support Program of Shanghai, the projects from Shanghai Science and Technology Commission (Grant No. 19JC1412200), the Program for Professor of Special Appointment (Eastern Scholar) at Shanghai Institutions of Higher Learning, the Shanghai Natural Science Foundation (Grant No. 22ZR1421400), and the Fundamental Research Funds for the Central Universities. Y.P. acknowledges the support from the CAS Key Technology Talent Program. All the authors acknowledge assistance from Dr. Long Zhao and Meng Yang from USTC. R.I.K. and J.M. thank the US National Science Foundation (NSF AST 2103269) to model the reflectron time-of-flight mass spectrometer.

■ REFERENCES

- Herbst, E.; Van Dishoeck, E. F. Complex Organic Interstellar Molecules. *Annu. Rev. Astron. Astr.* **2009**, *47*, 427–480.
- Boogert, A. A.; Gerakines, P. A.; Whittet, D. C. Observations of the Icy Universe. *Annu. Rev. Astron. Astr.* **2015**, *53*, 541–581.
- Agúndez, M.; Marcelino, N.; Tercero, B.; Cabezas, C.; de Vicente, P.; Cernicharo, J. O-Bearing Complex Organic Molecules at the Cyanopolyyne Peak of TMC-1: Detection of C_2H_3CHO , C_2H_3OH , $HCOOCH_3$, and CH_3OCH_3 . *Astron. Astrophys.* **2021**, *649*, L4.
- Öberg, K. I. Photochemistry and Astrochemistry: Photochemical Pathways to Interstellar Complex Organic Molecules. *Chem. Rev.* **2016**, *116*, 9631–9663.
- Sandford, S. A.; Nuevo, M.; Bera, P. P.; Lee, T. J. Prebiotic Astrochemistry and the Formation of Molecules of Astrobiological Interest in Interstellar Clouds and Protostellar Disks. *Chem. Rev.* **2020**, *120*, 4616–4659.
- Turner, A. M.; Kaiser, R. I. Exploiting Photoionization Reflectron Time-of-Flight Mass Spectrometry to Explore Molecular Mass Growth Processes to Complex Organic Molecules in Interstellar and Solar System Ice Analogs. *Acc. Chem. Res.* **2020**, *53*, 2791–2805.
- Duley, W. W.; Williams, D. A. *Interstellar Chemistry*; Academic Press: London, 1984.
- Hartquist, T. W.; Williams, D. A. *The Chemically Controlled Cosmos: Astronomical Molecules from the Big Bang to Exploding Stars*; Cambridge University Press: Cambridge, 1995.
- Cronin, J. R.; Pizzarello, S. Enantiomeric Excesses in Meteoritic Amino Acids. *Science* **1997**, *275*, 951–955.
- Glavin, D. P.; Burton, A. S.; Elsila, J. E.; Aponte, J. C.; Dworkin, J. P. The Search for Chiral Asymmetry as a Potential Biosignature in Our Solar System. *Chem. Rev.* **2020**, *120*, 4660–4689.
- Furukawa, Y.; Chikaraishi, Y.; Ohkouchi, N.; Ogawa, N. O.; Glavin, D. P.; Dworkin, J. P.; Abe, C.; Nakamura, T. Extraterrestrial Ribose and Other Sugars in Primitive Meteorites. *Proc. Natl. Acad. Sci. U. S. A.* **2019**, *116*, 24440–24445.
- Cronin, J. R.; Chang, S. Organic Matter in Meteorites: Molecular and Isotopic Analyses of the Murchison Meteorite. In *The Chemistry of Life's Origins*; Springer: Dordrecht, 1993.
- Herbst, E.; Yates, J. T., Jr. Introduction: Astrochemistry. *Chem. Rev.* **2013**, *113*, 8707–8709.

(14) Woon, D. E. Quantum Chemical Cluster Studies of Cation–Ice Reactions for Astrochemical Applications: Seeking Experimental Confirmation. *Acc. Chem. Res.* **2021**, *54*, 490–497.

(15) Bennett, C. J.; Chen, S.-H.; Sun, B.-J.; Chang, A. H.; Kaiser, R. I. Mechanical Studies on the Irradiation of Methanol in Extraterrestrial Ices. *Astrophys. J.* **2007**, *660*, 1588.

(16) Zhou, L.; Kaiser, R. I.; Gao, L. G.; Chang, A. H.; Liang, M.-C.; Yung, Y. L. Pathways to Oxygen-Bearing Molecules in the Interstellar Medium and in Planetary Atmospheres: Cyclopropenone ($c\text{-C}_3\text{H}_2\text{O}$) and Propynal (HCCCHO). *Astrophys. J.* **2008**, *686*, 1493.

(17) Öberg, K. I.; Garrod, R. T.; Van Dishoeck, E. F.; Linnartz, H. Formation Rates of Complex Organics in Uv Irradiated CH_3OH -Rich Ices-I. Experiments. *Astron. Astrophys.* **2009**, *504*, 891–913.

(18) Ruf, A.; Lange, J.; Eddhif, B.; Geffroy, C.; d'Hendecourt, L. L. S.; Poinot, P.; Danger, G. The Challenging Detection of Nucleobases from Pre-Accretional Astrophysical Ice Analogs. *Astrophys. J. Lett.* **2019**, *887*, L31.

(19) Materese, C. K.; Gerakines, P. A.; Hudson, R. L. Laboratory Studies of Astronomical Ices: Reaction Chemistry and Spectroscopy. *Acc. Chem. Res.* **2021**, *54*, 280–290.

(20) Zhu, C.; Turner, A. M.; Abplanalp, M. J.; Kaiser, R. I.; Webb, B.; Siuzdak, G.; Fortenberry, R. C. An Interstellar Synthesis of Glycerol Phosphates. *Astrophys. J. Lett.* **2020**, *899*, L3.

(21) Bennett, C. J.; Kaiser, R. I. On the Formation of Glycolaldehyde (HCOCH_2OH) and Methyl Formate (HCOOCH_3) in Interstellar Ice Analogs. *Astrophys. J.* **2007**, *661*, 899.

(22) Maity, S.; Kaiser, R. I.; Jones, B. M. Infrared and Reflectron Time-of-Flight Mass Spectroscopic Study on the Synthesis of Glycolaldehyde in Methanol (CH_3OH) and Methanol–Carbon Monoxide ($\text{CH}_3\text{OH}–\text{CO}$) Ices Exposed to Ionization Radiation. *Faraday Discuss.* **2014**, *168*, 485–516.

(23) de Marcellus, P.; Meinert, C.; Myrgorodska, I.; Nahon, L.; Buhse, T.; d'Hendecourt, L. L. S.; Meierhenrich, U. J. Aldehydes and Sugars from Evolved Precometary Ice Analogs: Importance of Ices in Astrochemical and Prebiotic Evolution. *Proc. Natl. Acad. Sci. U. S. A.* **2015**, *112*, 965–970.

(24) Kleimeier, N. F.; Eckhardt, A. K.; Kaiser, R. I. Identification of Glycolaldehyde Enol ($\text{HOHC}=\text{CHOH}$) in Interstellar Analogue Ices. *J. Am. Chem. Soc.* **2021**, *143*, 14009–14018.

(25) Bernstein, M. P.; Dworkin, J. P.; Sandford, S. A.; Cooper, G. W.; Allamandola, L. J. Racemic Amino Acids from the Ultraviolet Photolysis of Interstellar Ice Analogs. *Nature* **2002**, *416*, 401–403.

(26) Munoz Caro, G.; Meierhenrich, U. J.; Schutte, W. A.; Barbier, B.; Arcones Segovia, A.; Rosenbauer, H.; Thiemann, W.-P.; Brack, A.; Greenberg, J. M. Amino Acids from Ultraviolet Irradiation of Interstellar Ice Analogs. *Nature* **2002**, *416*, 403–406.

(27) Holtom, P. D.; Bennett, C. J.; Osamura, Y.; Mason, N. J.; Kaiser, R. I. A Combined Experimental and Theoretical Study on the Formation of the Amino Acid Glycine ($\text{NH}_2\text{CH}_2\text{COOH}$) and Its Isomer (CH_3NHCOOH) in Extraterrestrial Ices. *Astrophys. J.* **2005**, *626*, 940.

(28) Kaiser, R.; Stockton, A.; Kim, Y.; Jensen, E.; Mathies, R. On the Formation of Dipeptides in Interstellar Model Ices. *Astrophys. J.* **2013**, *765*, 111.

(29) Oba, Y.; Takano, Y.; Naraoka, H.; Watanabe, N.; Kouchi, A. Nucleobase Synthesis in Interstellar Ices. *Nat. Commun.* **2019**, *10*, 4413.

(30) Turner, A. M.; Abplanalp, M. J.; Blair, T. J.; Dayuha, R.; Kaiser, R. I. An Infrared Spectroscopic Study toward the Formation of Alkylphosphonic Acids and Their Precursors in Extraterrestrial Environments. *Astrophys. J. Suppl. S.* **2018**, *234*, 6.

(31) Turner, A. M.; Abplanalp, M. J.; Bergantini, A.; Frigge, R.; Zhu, C.; Sun, B.-J.; Hsiao, C.-T.; Chang, A. H.; Meinert, C.; Kaiser, R. I. Origin of Alkylphosphonic Acids in the Interstellar Medium. *Sci. Adv.* **2019**, *5*, eaaw4307.

(32) Williams, D. A.; Hartquist, T. W. The Chemistry of Star-Forming Regions. *Acc. Chem. Res.* **1999**, *32*, 334–341.

(33) Herbst, E. The Chemistry of Interstellar Space. *Chem. Soc. Rev.* **2001**, *30*, 168–176.

(34) Williams, D. A.; Herbst, E. It's a Dusty Universe: Surface Science in Space. *Surf. Sci.* **2002**, *500*, 823–837.

(35) Aikawa, Y. Interplay of Chemistry and Dynamics in the Low-Mass Star Formation. *Chem. Rev.* **2013**, *113*, 8961–8980.

(36) Gudipati, M. S.; Allamandola, L. J. Facile Generation and Storage of Polycyclic Aromatic Hydrocarbon Ions in Astrophysical Ices. *Astrophys. J.* **2003**, *596*, L195.

(37) Abplanalp, M. J.; Frigge, R.; Kaiser, R. I. Low-Temperature Synthesis of Polycyclic Aromatic Hydrocarbons in Titan's Surface Ices and on Airless Bodies. *Sci. Adv.* **2019**, *5*, eaaw5841.

(38) Urso, R.; Scirè, C.; Baratta, G.; Compagnini, G.; Palumbo, M. E. Combined Infrared and Raman Study of Solid CO. *Astron. Astrophys.* **2016**, *594*, A80.

(39) Bennett, C. J.; Brotton, S. J.; Jones, B. M.; Misra, A. K.; Sharma, S. K.; Kaiser, R. I. High-Sensitivity Raman Spectrometer to Study Pristine and Irradiated Interstellar Ice Analogs. *Anal. Chem.* **2013**, *85*, S659–S665.

(40) Baratta, G.; Brunetto, R.; Leto, G.; Palumbo, M.; Spinella, F.; Strazzulla, G. Raman Spectroscopy of Ion-Irradiated Astrophysically Relevant Materials. *J. Raman Spectrosc.* **2008**, *39*, 211–219.

(41) Chuang, K.-J.; Fedoseev, G.; Ioppolo, S.; Van Dishoeck, E.; Linnartz, H. H-Atom Addition and Abstraction Reactions in Mixed CO, H_2CO and CH_3OH Ices—an Extended View on Complex Organic Molecule Formation. *Mon. Not. R. Astron. Soc.* **2016**, *455*, 1702–1712.

(42) Fedoseev, G.; Chuang, K.-J.; Ioppolo, S.; Qasim, D.; van Dishoeck, E. F.; Linnartz, H. Formation of Glycerol through Hydrogenation of CO Ice under Prestellar Core Conditions. *Astrophys. J.* **2017**, *842*, 52.

(43) Zhu, C.; Turner, A. M.; Abplanalp, M. J.; Kaiser, R. I. Formation of High-Order Carboxylic Acids (RCOOH) in Interstellar Analogous Ices of Carbon Dioxide (CO_2) and Methane (CH_4). *Astrophys. J. Suppl. S.* **2018**, *234*, 15.

(44) Yocum, K. M.; Smith, H. H.; Todd, E. W.; Mora, L.; Gerakines, P. A.; Milam, S. N.; Widicus Weaver, S. L. Millimeter/Submillimeter Spectroscopic Detection of Desorbed Ices: A New Technique in Laboratory Astrochemistry. *J. Phys. Chem. A* **2019**, *123*, 8702–8708.

(45) Yocum, K.; Milam, S.; Gerakines, P.; Weaver, S. W. Sublimation of Laboratory Ices Millimeter/Submillimeter Experiment (SubLIME): Structure-Specific Identifications of Products from UV-Photolyzed Methanol Ice. *Astrophys. J.* **2021**, *913*, 61.

(46) Jones, B. M.; Kaiser, R. I. Application of Reflectron Time-of-Flight Mass Spectroscopy in the Analysis of Astrophysically Relevant Ices Exposed to Ionization Radiation: Methane (CH_4) and D_4 -Methane (CD_4) as a Case Study. *J. Phys. Chem. Lett.* **2013**, *4*, 1965–1971.

(47) Kaiser, R. I.; Maity, S.; Jones, B. M. Synthesis of Prebiotic Glycerol in Interstellar Ices. *Angew. Chem., Int. Ed.* **2015**, *54*, 195–200.

(48) Abplanalp, M. J.; Gozem, S.; Krylov, A. I.; Shingledecker, C. N.; Herbst, E.; Kaiser, R. I. A Study of Interstellar Aldehydes and Enols as Tracers of a Cosmic Ray-Driven Nonequilibrium Synthesis of Complex Organic Molecules. *Proc. Natl. Acad. Sci. U. S. A.* **2016**, *113*, 7727–7732.

(49) Turner, A. M.; Bergantini, A.; Abplanalp, M. J.; Zhu, C.; Góbi, S.; Sun, B.-J.; Chao, K.-H.; Chang, A. H.; Meinert, C.; Kaiser, R. I. An Interstellar Synthesis of Phosphorus Oxoacids. *Nat. Commun.* **2018**, *9*, 3851.

(50) Zhu, C.; Bergantini, A.; Singh, S. K.; Abplanalp, M. J.; Kaiser, R. I. Rapid Radical–Radical Induced Explosive Desorption of Ice-Coated Interstellar Nanoparticles. *Astrophys. J.* **2021**, *920*, 73.

(51) Zhu, C.; Kleimeier, N. F.; Turner, A. M.; Singh, S. K.; Fortenberry, R. C.; Kaiser, R. I. Synthesis of Methanediol [$\text{CH}_2(\text{OH})_2$]: The Simplest Geminal Diol. *Proc. Natl. Acad. Sci.* **2022**, *119*, e2111938119.

(52) Bennett, C. J.; Jamieson, C. S.; Kaiser, R. I. Mechanical Studies on the Formation of Carbon Dioxide in Extraterrestrial Carbon Monoxide Ice Analog Samples. *Phys. Chem. Chem. Phys.* **2009**, *11*, 4210–4218.

(53) Bennett, C. J.; Jamieson, C. S.; Kaiser, R. I. Mechanical Studies on the Formation and Destruction of Carbon Monoxide (CO), Carbon Dioxide (CO₂), and Carbon Trioxide (CO₃) in Interstellar Ice Analog Samples. *Phys. Chem. Chem. Phys.* **2010**, *12*, 4032–4050.

(54) Zhu, C.; Eckhardt, A. K.; Chandra, S.; Turner, A. M.; Schreiner, P. R.; Kaiser, R. I. Identification of a Prismatic P₃N₃ Molecule Formed from Electron Irradiated Phosphine-Nitrogen Ices. *Nat. Commun.* **2021**, *12*, 5467.

(55) Kaiser, R. I.; Hansen, N. An Aromatic Universe—a Physical Chemistry Perspective. *J. Phys. Chem. A* **2021**, *125*, 3826–3840.

(56) Qi, F. Combustion Chemistry Probed by Synchrotron VUV Photoionization Mass Spectrometry. *P. Combust. Inst.* **2013**, *34*, 33–63.

(57) Sarathy, S. M.; Oßwald, P.; Hansen, N.; Kohse-Höinghaus, K. Alcohol Combustion Chemistry. *Prog. Energy Combust.* **2014**, *44*, 40–102.

(58) Jiao, F.; Li, J.; Pan, X.; Xiao, J.; Li, H.; Ma, H.; Wei, M.; Pan, Y.; Zhou, Z.; Li, M.; et al. Selective Conversion of Syngas to Light Olefins. *Science* **2016**, *351*, 1065–1068.

(59) Yeghikyan, A. Irradiation of Dust in Molecular Clouds. II. Doses Produced by Cosmic Rays. *Astrophys.* **2011**, *54*, 87–99.

(60) Cool, T. A.; Nakajima, K.; Mostafaoui, T. A.; Qi, F.; McIlroy, A.; Westmoreland, P. R.; Law, M. E.; Poisson, L.; Peterka, D. S.; Ahmed, M. Selective Detection of Isomers with Photoionization Mass Spectrometry for Studies of Hydrocarbon Flame Chemistry. *J. Chem. Phys.* **2003**, *119*, 8356–8365.

(61) Yang, B.; Wang, J.; Cool, T. A.; Hansen, N.; Skeen, S.; Osborn, D. L. Absolute Photoionization Cross-Sections of Some Combustion Intermediates. *Int. J. Mass Spectrom.* **2012**, *309*, 118–128.

(62) Chupka, W. A. Factors Affecting Lifetimes and Resolution of Rydberg States Observed in Zero-Electron-Kinetic-Energy Spectroscopy. *J. Chem. Phys.* **1993**, *98*, 4520–4530.

(63) Bergantini, A.; Abplanalp, M. J.; Pokhilko, P.; Krylov, A. I.; Shingledecker, C. N.; Herbst, E.; Kaiser, R. I. A Combined Experimental and Theoretical Study on the Formation of Interstellar Propylene Oxide (CH₃CHCH₂O) — a Chiral Molecule. *Astrophys. J.* **2018**, *860*, 108.

(64) Zhu, C.; Frigge, R.; Bergantini, A.; Fortenberry, R. C.; Kaiser, R. I. Untangling the Formation of Methoxymethanol (CH₃OCH₂OH) and Dimethyl Peroxide (CH₃OOCH₃) in Star-Forming Regions. *Astrophys. J.* **2019**, *881*, 156.

(65) Mallard, W. NIST Chemistry Webbook, NIST Standard Reference Database. <http://webbook.nist.gov/>; 2000, 69.

(66) Turner, A. M.; Koutsogiannis, A. S.; Kleimeier, N. F.; Bergantini, A.; Zhu, C.; Fortenberry, R. C.; Kaiser, R. I. An Experimental and Theoretical Investigation into the Formation of Ketene (H₂CCO) and Ethynol (HCCOH) in Interstellar Analog Ices. *Astrophys. J.* **2020**, *896*, 88.

(67) Manigand, S.; Jørgensen, J.; Calcutt, H.; Müller, H.; Ligterink, N. F. W.; Coutens, A.; Drozdovskaya, M. N.; van Dishoeck, E.; Wampfler, S. The Alma-Pils Survey: Inventory of Complex Organic Molecules Towards IRAS 16293–2422 A. *Astron. Astrophys.* **2020**, *635*, A48.

(68) Öberg, K. I.; Guzmán, V. V.; Walsh, C.; Aikawa, Y.; Bergin, E. A.; Law, C. J.; Loomis, R. A.; Alarcón, F.; Andrews, S. M.; Bae, J.; et al. Molecules with Alma at Planet-Forming Scales (MAPS). I. Program Overview and Highlights. *Astrophys. J. Suppl. S.* **2021**, *257*, 1.

(69) Turner, A. M.; Abplanalp, M. J.; Chen, S. Y.; Chen, Y. T.; Chang, A. H.; Kaiser, R. I. A Photoionization Mass Spectroscopic Study on the Formation of Phosphanes in Low Temperature Phosphine Ices. *Phys. Chem. Chem. Phys.* **2015**, *17*, 27281–27291.

(70) Drouin, D.; Couture, A. R.; Joly, D.; Tastet, X.; Aimez, V.; Gauvin, R. Casino V2.42 - a Fast and Easy-to-Use Modeling Tool for Scanning Electron Microscopy and Microanalysis Users. *Scanning* **2007**, *29*, 92–101.

□ Recommended by ACS

Size-Resolved Chemical Composition of Sub-20 nm Particles from Methanesulfonic Acid Reactions with Methylamine and Ammonia

Véronique Perraud, James N. Smith, et al.

JUNE 24, 2020

ACS EARTH AND SPACE CHEMISTRY

READ □

Sampling Accelerated Micron Scale Ice Particles with a Quadrupole Ion Trap Mass Spectrometer

Anton Belousov, Morgan Cable, et al.

APRIL 01, 2021

JOURNAL OF THE AMERICAN SOCIETY FOR MASS SPECTROMETRY

READ □

Chemical Imaging of Atmospheric Particles

Alexander Laskin, Mary K. Gilles, et al.

NOVEMBER 12, 2019

ACCOUNTS OF CHEMICAL RESEARCH

READ □

On the Complementarity and Informative Value of Different Electron Ionization Mass Spectrometric Techniques for the Chemical Analysis of Secondary...

Elena Hartner, Ralf Zimmermann, et al.

MAY 06, 2022

ACS EARTH AND SPACE CHEMISTRY

READ □

Get More Suggestions >